# Journal of Applied Sciences

ISSN 1812-5654

science alert

ANSInet
an open access publisher
http://ansinet.com

OPEN ACCESS Journal of Applied Sciences

ISSN 1812-5654
DOI: 10.3923/jas.2017.315.323

# Research Article
# Heat Transfer and Liquid Distribution Between Two Moving Porous Surfaces

[1]Médard Marcus Nganbe II, [1]Jacques Hona, [2]Elisabeth Ngo Nyobe and [1]Elkana Pemha

[1]Applied Mechanics Laboratory, Faculty of Science, University of Yaoundé I, P.O. Box 7389, Yaoundé, Cameroon
[2]Department of Mathematics and Physical Science, National Advanced School of Engineering, University of Yaoundé I, P.O. Box 8390, Yaoundé, Cameroon

## Abstract

**Background and Objective:** Fluid flow and heat transfer between two permeable walls are used to model a variety of porous surface mechanisms ubiquitous in engineering and industry. This study deals with a numerical contribution in order to ensure a deeper understanding of phenomena of heat and mass distributions inside a rectangular, porous industrial conduct. The investigation is restricted to find a numerical solution of a two-dimensional flow driven by liquid withdrawal/addition also known as suction/injection through two parallel porous walls which are accelerated and maintained at different temperatures. **Materials and Methods:** By similarity transformation, the Navier-Stokes equations and the energy equation describing mass and heat distributions inside the channel are reduced to a nonlinear boundary-value problem which is solved applying a numerical integration based on the shooting method. **Results:** The solution of the problem is expressed in terms of velocity components, temperature and pressure gradients between two opposing permeable surfaces. **Conclusion:** It is found that positive wall accelerating parameters give the existence of flow reversal. Boundary layers occur inside the channel with the growth of the injection Reynolds number at a fixed positive accelerating parameter and by increasing the suction Reynolds number in the case of a fixed negative accelerating parameter. Thermal boundary layers take place within the channel when the Péclet number approaches the values of 10 and -10 at fixed positive and negative accelerating parameters, respectively.

Key words: Injection/suction-driven flow, heat transfer, similarity solutions, nonlinear boundary-value problem, numerical results

Received: November 16, 2016 Accepted: February 06, 2017 Published: May 15, 2017

Citation: Médard Marcus Nganbe II, Jacques Hona, Elisabeth Ngo Nyobe and Elkana Pemha, 2017. Heat transfer and liquid distribution between two moving porous surfaces. J. Applied Sci., 17: 315-323.

Corresponding Author: Jacques Hona, Applied Mechanics Laboratory, Faculty of Science, University of Yaoundé I, P.O. Box 7389, Yaoundé, Cameroon



Competing Interest: The authors have declared that no competing interest exists.

Data Availability: All relevant data are within the paper and its supporting information files.

## INTRODUCTION

Heat and mass distributions in industrial systems are increasingly controlled using numerical approaches[1-3]. Fluid flow within a porous channel is related to several applications including filtration in petroleum industry, biopharmaceutical industry and in water industry[4,5]. Many scientists interested to characterize the phenomenon of fluid distribution in a two-dimensional channel use the solutions of the Navier-Stokes equations.

Two types of geometrical configurations of the flow are often encountered in industrial fluid dynamics, so the channel may be rectangular or cylindrical. The dynamics of the fluid is described relative to both geometrical configurations by interpreting the solutions of the Navier-Stokes equations. The Navier-Stokes equations for rectangular channel flows with fixed porous walls are usually solved applying a similarity method first introduced by Berman[6] and extended by other authors[7-9]. The theory of normal modes which is another type of similarity method helps to investigate the temporal and the spatial stabilities of steady-state solutions of the Navier-Stokes equations[9-12]. The method of similarity solution is also used to investigate the flows through cylindrical conducts[13-15].

Studies of fluid flows incorporating thermal effects in the both rectangular and cylindrical configurations using the similarity approach reveal many rich hydrodynamic structures[16-20]. In many cases, the flow is driven by suction or injection through channels or tubes with fixed porous walls. The consideration of the motion of the porous walls gives rise to other interesting studies. In fact, the porous walls can move orthogonally to the streamwise direction of the flow in order to model slab rocket motors[15,21]. The problem of the porous walls which move parallel to the streamwise direction with heat transfer considering temperature-dependent thermal conductivity is discussed in the present investigation.

In validating the similarity solutions recounted above, investigators have often relied on numerical simulations. Extensive experimental verifications have also been accomplished. In fact, numerous laboratory experiments on porous channel flows have been conducted by many authors[4,7,9,11].

The present study was aimed to highlight hydrodynamic structures in terms of velocity components, pressure gradients and temperature inside a symmetric channel with two equally accelerating porous walls maintained at different temperatures. To ensure a better understanding of the flow and heat transfer under study, the mathematical model of the problem applying a similarity transformation technique is provided before the presentation and the discussion of numerical results. The conclusion contains the main findings of the study.

## MATERIALS AND METHODS

An incompressible viscous fluid is in motion through two horizontal porous walls distanced by 2a as shown in Fig. 1. The origin is placed in the center of the channel and the length of the porous walls measured in the streamwise direction is taken to be greater than the width 2a. Despite the porous wall finite length in the streamwise direction, it is common place to assume infinite length in order to neglect the influence of the opening at the ends[15,21]. The channel is built on the base of a plane Cartesian coordinate system (x, y), where x is the axial or the streamwise coordinate; y denotes the transverse or the normal coordinate. The flow is assumed to be two-dimensional, so the velocity field has components as $(V_x, V_y)$, where $V_x$ is the streamwise or the axial velocity and $V_y$ is the transverse or the normal velocity. The two porous walls are accelerated along the streamwise direction, such that the velocity of fluid particles at walls $V_x = Ex$, varies linearly with

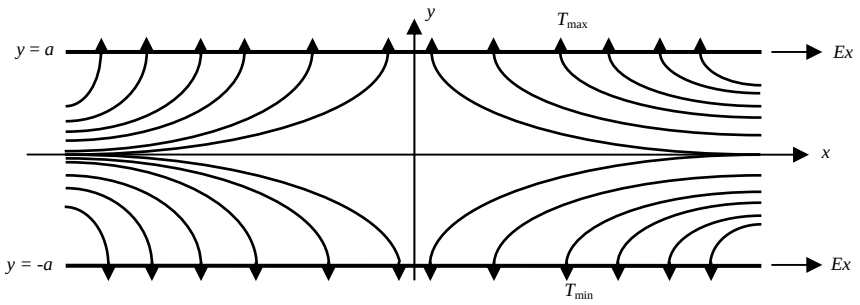


Fig. 1: Geometry of the channel showing the difference of temperature between the two accelerating porous walls. The plotted streamlines represent the flow pattern of a symmetric similarity solution of the Navier-Stokes equations for the suction problem

the position x, where the quantity E is proportional to the wall moving strength and its unit is 1/s. The temperature of the cold wall situated at y = -a is $T_{min}$ and that of the hot wall located at y = +a is $T_{max}$. The rectangular channel admits a midsection plane at y = 0 known as the open wall dividing the flow domain into two identical parts. The variables describing pressure and temperature within the channel are p and T, respectively. Equal fluxes are established at boundaries with V the fluid speed at walls positive for injection but negative for suction. The constant physical properties of the fluid are the specific mass ρ and the dynamic viscosity μ. Temperature-dependent thermal conductivity is k and its value $k_0$ at temperature $T_{min}$ is taken as a reference value.

In the absence of body forces due to the fact that the channel is horizontal and neglecting dissipation effects which could occur inside the flow domain, the equations of motion are obtained by applying the conservations of mass, momentum and energy as in the following equations:

$$\frac{\partial V_x}{\partial x}+\frac{\partial V_y}{\partial y}=0 \tag{1}$$

$$\rho\left(V_x\frac{\partial V_x}{\partial x}+V_y\frac{\partial V_x}{\partial y}\right)=-\frac{\partial p}{\partial x}+\mu\left(\frac{\partial^2 V_x}{\partial x^2}+\frac{\partial^2 V_x}{\partial y^2}\right) \tag{2}$$

$$\rho\left(V_x\frac{\partial V_y}{\partial x}+V_y\frac{\partial V_y}{\partial y}\right)=-\frac{\partial p}{\partial y}+\mu\left(\frac{\partial^2 V_y}{\partial x^2}+\frac{\partial^2 V_y}{\partial y^2}\right) \tag{3}$$

$$\rho\left(V_x\frac{\partial T}{\partial x}+V_y\frac{\partial T}{\partial y}\right)=\frac{\partial}{\partial x}\left(k\frac{\partial T}{\partial x}\right)+\frac{\partial}{\partial y}\left(k\frac{\partial T}{\partial y}\right) \tag{4}$$

where, mass conservation is described by the continuity Eq. 1, momentum conservation or the momentum equation consists of the two Navier-Stokes Eq. 2 and 3, energy conservation is described by Eq. 4. Taking into account the geometrical configuration of the problem, the boundary conditions are given by:

$$\begin{array}{llll} V_x=Ex, & V_y=-V, & T=T_{max} & \text{for } y=a \\ \frac{\partial V_x}{\partial y}=0, & V_y=0, & T=T_{max}/2 & \text{for } y=0 \\ V_x=Ex, & V_y=V, & T=T_{min}=0 & \text{for } y=-a \end{array} \tag{5}$$

The boundary conditions at y = ±a, express the temperature of the hot wall $T_{max}$, that of the cold wall $T_{min}$, the fluid injection/suction speed $V_y = \pm V$ and the velocity of the walls $V_x = Ex$. More precisely, the walls which move parallel to the streamwise direction are accelerated as their velocity varies with the position x. The boundary conditions, $\frac{\partial V_x}{\partial y}=0,\ V_y=0$ for y = 0 establish the symmetry inside the channel with respect to the midsection plane, also known as the open wall at temperature $T_{max}/2$.

It is convenient at this stage to generate some control parameters which help in discussing the dynamic behavior of the flow under study. These control numbers derive from the nondimensional formulation of the governing equations of the problem. Indeed, dimensionless variables for lengths, velocity components, pressure, temperature and thermal conductivity are introduced as follows:

$$\chi=\frac{x}{a},\ \eta=\frac{y}{a},\ u=\frac{V_x}{Ea+V},\ v=\frac{V_y}{Ea+V},\ \Pi=\frac{p}{\rho(Ea+V)^2},\ C=\frac{T}{T_{max}},\ \kappa=\frac{k}{k_0} \tag{6}$$

The governing equations written in terms of the above dimensionless variables become:

$$\frac{\partial u}{\partial \chi}+\frac{\partial v}{\partial \eta}=0 \tag{7}$$

$$u\frac{\partial u}{\partial \chi}+v\frac{\partial u}{\partial \eta}=-\frac{\partial \Pi}{\partial \chi}+\frac{1}{R}\left(\frac{\partial^2 u}{\partial \chi^2}+\frac{\partial^2 u}{\partial \eta^2}\right) \tag{8}$$

$$u\frac{\partial v}{\partial \chi}+v\frac{\partial v}{\partial \eta}=-\frac{\partial \Pi}{\partial \eta}+\frac{1}{R}\left(\frac{\partial^2 v}{\partial \chi^2}+\frac{\partial^2 v}{\partial \eta^2}\right) \tag{9}$$

$$u\frac{\partial C}{\partial \chi}+v\frac{\partial C}{\partial \eta}=\frac{1}{P}\left(\frac{\partial}{\partial \chi}\left(\kappa\frac{\partial C}{\partial \chi}\right)+\frac{\partial}{\partial \eta}\left(\kappa\frac{\partial C}{\partial \eta}\right)\right) \tag{10}$$

where, the Reynolds number R = ρ (Ea+V)a/μ and the Péclet number P = ρ (Ea+V)a/$k_0$ assumed positive for injection and negative for suction are introduced. The boundary conditions associated with Eq. 7-10 are derived:

$$\begin{array}{llll} u=\gamma\chi & v=\gamma-1, & C=1 & \text{for } \eta=1 \\ \frac{\partial u}{\partial \eta}=0, & v=0, & C=0.5 & \text{for } \eta=0 \\ u=\gamma\chi, & v=-(\gamma-1), & C=0 & \text{for } \eta=-1 \end{array} \tag{11}$$

The dimensionless quantity γ = Ea/(Ea + V) is the wall accelerating parameter. It is important at this stage to note that γ<0 corresponds to decelerating porous walls, while γ>0 deals with accelerating porous walls and γ = 1 is the case of a channel flow with accelerating walls in the absence of porosity. In addition, γ = 0 corresponds to fixed porous walls.

The incompressibility of the fluid gives the existence of a stream function f φ. The prescription of the stream function into the governing equations is accompanied by a new function Ω describing the energy distribution. In addition, to complete the statement of the problem, a functional dependence of nondimensional thermal conductivity on temperature κ(Ω) is required. Thus, the following transformations are adopted:

$$\begin{aligned}
&\varphi(\chi,\eta) = \chi\psi(\eta)\\
&u(\chi,\eta) = \frac{\partial\varphi}{\partial\eta} = \chi\psi^{(1)}(\eta)\\
&v(\chi,\eta) = -\frac{\partial\varphi}{\partial\chi} = -\psi(\eta)\\
&C(\chi,\eta) = \Omega(\eta)\\
&\kappa(\Omega) = 1+\beta\Omega
\end{aligned} \tag{12}$$

where, ψ denotes the stream function per unit length and $\psi^{(1)} = d\psi/d\eta$. The non dimensional parameter $\beta = d\kappa/d\Omega$ depends on the fluid properties and on the temperature difference between the walls and is a measure of the sensitivity of thermal conductivity to the variations of temperature. Equation 12 derived from a similarity technique to solve the differential Eq. 7-11. However, other methods to find the solutions of the Navier-Stokes equations and the energy equation exist. Indeed, another approach could consist to determine the velocity components and temperature directly without introducing functions ψ and Ω. In the present study, the solutions are the ones that assume that the similarity properties (Eq. 12) are satisfied and the objective of this study is only to analyze solutions given by the transformations (Eq. 12).

Applying the similarity properties (Eq. 12), the non dimensional continuity Eq. 7 is self satisfied. By taking the curl of the momentum equation, function ψ satisfies the vorticity transport equation, while function Ω describes the similarity energy equation as follows:

$$\psi^{(4)} + R\left(\psi\psi^{(3)} - \psi^{(1)}\psi^{(2)}\right) = 0 \tag{13}$$

$$(1+\beta\Omega)\Omega^{(2)} + \beta(\Omega^{(1)})^2 + P\psi\Omega^{(1)} = 0 \tag{14}$$

The boundary conditions corresponding to functions ψ and Ω are given:

$$\begin{array}{lll}
\psi^{(1)}(1) = \gamma, & \psi(1) = -(\gamma-1), & \Omega(1) = 1\\
\psi^{(2)}(2) = 0, & \psi(1) = 1, & \Omega(0) = 0.5\\
\psi^{(1)}(-1) = \gamma, & \psi(-1) = \gamma-1, & \Omega(-1) = 0
\end{array} \tag{15}$$

with $\psi^{(i)} = d^i\psi/d\eta^i$ and $\Omega^{(i)} = d^i\Omega/d\eta^i$. Equation 13-15 represent a nonlinear boundary-value problem. Pressure terms which have disappeared while taking the curl of the momentum equation, can now be yielded by introducing the similarity properties (Eq. 12) into Eq. 8 and 9. These pressure terms are given by:

$$A = \frac{1}{\chi}\frac{\partial\Pi}{\partial\chi} = \frac{1}{R}\psi^{(3)} + \psi\psi^{(2)} - \left(\psi^{(1)}\right)^2 = \text{constant} \tag{16}$$

$$Q(\eta) = \frac{\partial\Pi}{\partial\eta} = -\frac{1}{R}\psi^{(2)} - \psi\psi^{(1)} \tag{17}$$

It appears that the axial pressure gradient per unit length *A* as expressed in Eq. 16 is constant through the channel since it is equivalent to the integral of the left hand side of the vorticity (Eq. 13) at a given Reynolds number. Thus, a major attention is focused on the transverse pressure gradient Q defined in Eq. 17.

## RESULTS AND DISCUSSION

The rapidly converging shooting method[20,21] is used to obtain the numerical solution of the problem defined through Eq. 13-15. Since the channel admits a midsection plane at η = 0, the numerical integration is performed in two stages. The first stage consists to find the solutions on the interval [-1, 0] and the second stage is about the solutions relative to the interval [0, 1]. In each stage, a coupled nonlinear two-point boundary-value problem is solved between an open wall at η = 0 and a rigid accelerating porous wall at η = ±1 as shown through the boundary conditions. By combining results of the two stages, the complete solution corresponding to the interval [-1, 1] is derived.

The effects of positive and negative values of the accelerating parameter on the streamwise velocity per unit length u/χ are compared in Fig. 2a. Indeed, when the parameter γ is positive, the flow is completely reversed around the center of the channel in the cases of suction and injection. More precisely, flow reversal is a phenomenon where the velocity is in the opposite direction to the primary flow. In this study, the velocity primarily obeys u/χ > 0, so the reverse corresponds to instances where u/χ<0. On the other hand, the suction or the mass withdrawal phenomenon is characterized by negative values of the Reynolds number, while positive values of R deal with injection or the mass addition process within the channel.

With the increase of the injection Reynolds number at a fixed positive γ, the reverse flow is reduced around the middle

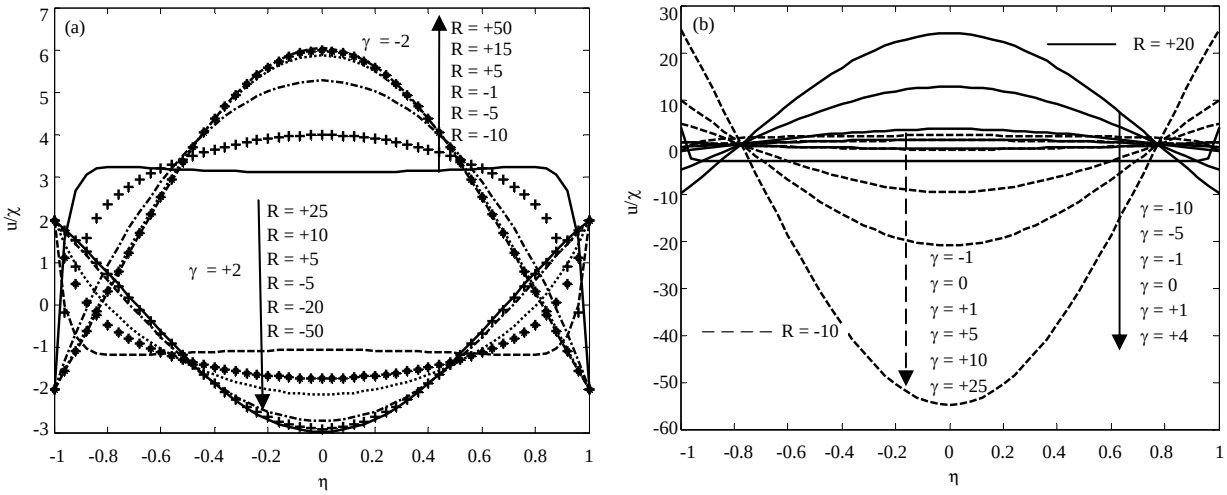


Fig. 2(a-b): Streamwise velocity per unit length, (a) At fixed positive and negative wall accelerating parameters for various Reynolds numbers and (b) At fixed injection and suction Reynolds numbers for various values of the wall accelerating parameter

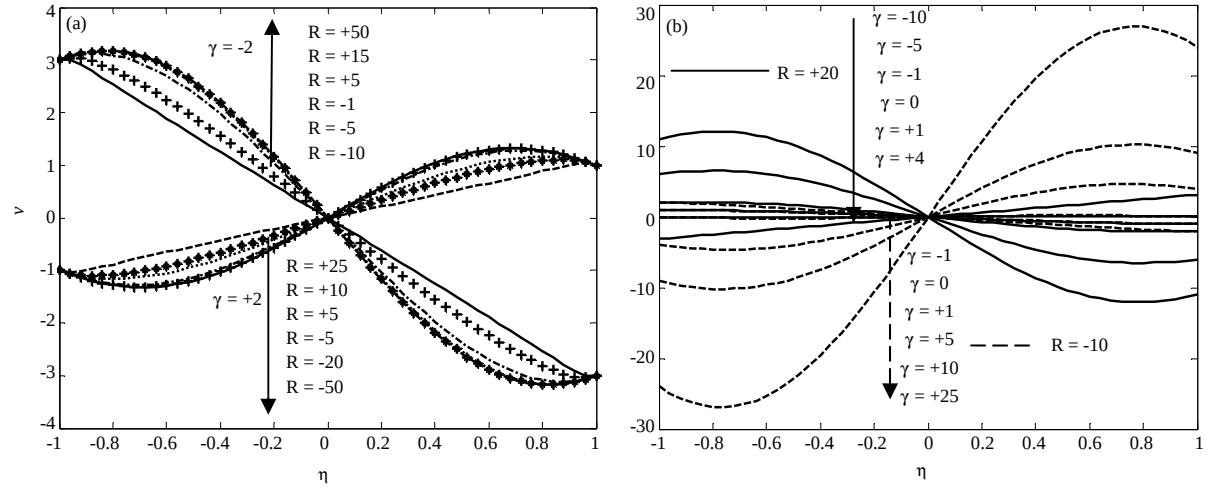


Fig. 3(a-b): Normal velocity, (a) At fixed positive and negative wall accelerating parameters for various Reynolds numbers and (b) At fixed injection and suction Reynolds numbers for various values of the wall accelerating parameter

of the flow domain and a boundary layer takes place. More precisely, at a fixed positive accelerating parameter, the dynamics of the fluid begins with a reverse type flow to a typical boundary layer type flow when the Reynolds number increases as found by Fang and Zhang[22] while studying a viscous flow between two stretchable disks in the absence of wall permeation. For a negative fixed parameter $\gamma$, Fig. 2a shows that the backward flow disappears in the neighborhood of the middle of the flow field and a boundary layer takes place by increasing the suction Reynolds number. The similar behavior revealed in the distribution of the streamwise velocity per unit length both for positive and negative accelerating parameters is that, function $u/\chi$ increases with the growth of the Reynolds number in the neighborhood of the center of the channel but decreases near the walls.

The effects of fixed suction and injection Reynolds numbers for different values of the accelerating parameter $\gamma$ on the streamwise velocity per unit length are superposed in Fig. 2b. In this figure, boundary layers appear by increasing $\gamma$ in the case of a fixed injection Reynolds number and by decreasing $\gamma$ for a fixed suction Reynolds number. In addition, for fixed suction and injection, the streamwise velocity per unit length decreases with the growth of the parameter $\gamma$ around the middle of the flow domain but increases in the neighborhood of the walls.

The normal velocity as plotted in Fig. 3a presents some regions where it exceeds its values at walls. In these regions,

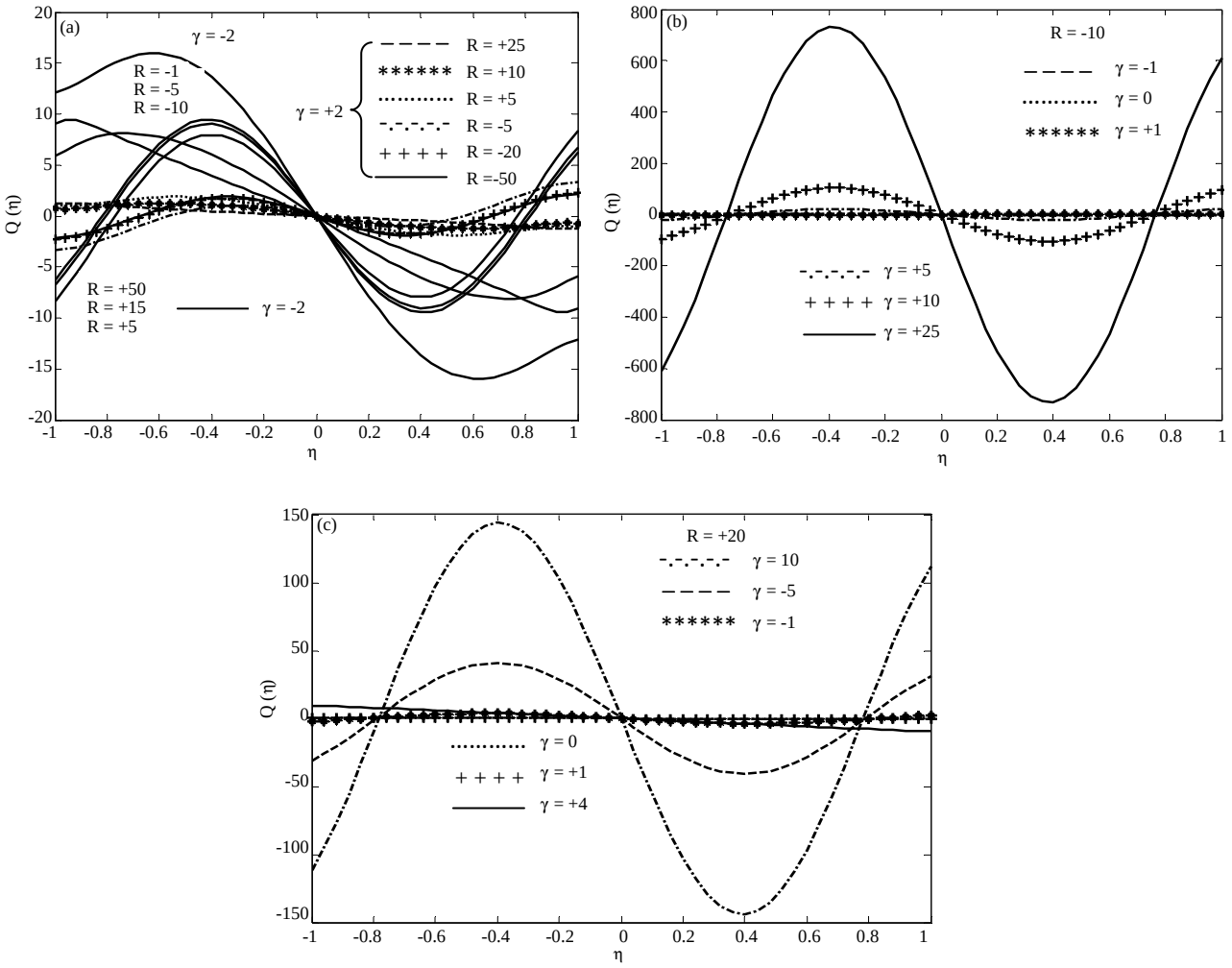


Fig. 4(a-c): Normal pressure gradient, (a) At fixed positive and negative wall accelerating parameters for various Reynolds numbers, (b) In the case of suction-driven flow for various values of the wall accelerating parameter and (c) In the case of injection-driven flow for various values of the wall accelerating parameter

the normal velocity overshoots as described in the studies of Brady[23] and Majdalani and Zhou[24]. These regions take place by increasing the suction Reynolds number at a fixed positive parameter *g* when flow reversal is dominant in the center of the channel and by increasing the injection Reynolds number at a fixed negative accelerating parameter. In the case-at-hand, when the boundary layer occurs at a positive fixed parameter $\gamma = +2$, Fig. 3a shows that the normal velocity approaches its expected law for an inviscid injection flow ($v = \eta$)[25,26] and for an inviscid suction flow at a negative fixed accelerating parameter $\gamma = -2$ ($v = -3\eta$). It follows that, the normal velocity reveals a linear law with the appearance of the boundary layer.

At fixed suction and injection Reynolds numbers, the normal velocity takes different values near the walls for various parameters $\gamma$ as shown in Fig. 3b. This figure also highlights the fact that great variations of function *v* occur in the case of suction at positive values of $\gamma$ and in the case of injection at negative values of the accelerating parameter.

The normal pressure gradient as presented in Fig. 4a is very sensitive to a negative fixed accelerating parameter which causes important variations of function $Q(\eta)$ compared to those observed in the case of a positive fixed g for different values of the Reynolds number. In addition, the normal pressure gradient reveals an oscillatory behavior within the channel which disappears with the appearance of the boundary layer. This behavior is in accordance with the velocity distribution due to momentum conservation. The comparison of the effects of fixed suction and injection Reynolds numbers on the normal pressure gradient as the parameter $\gamma$ takes different values is made in Fig. 4b, c. These figures show that, the boundary layer tends to cancel function

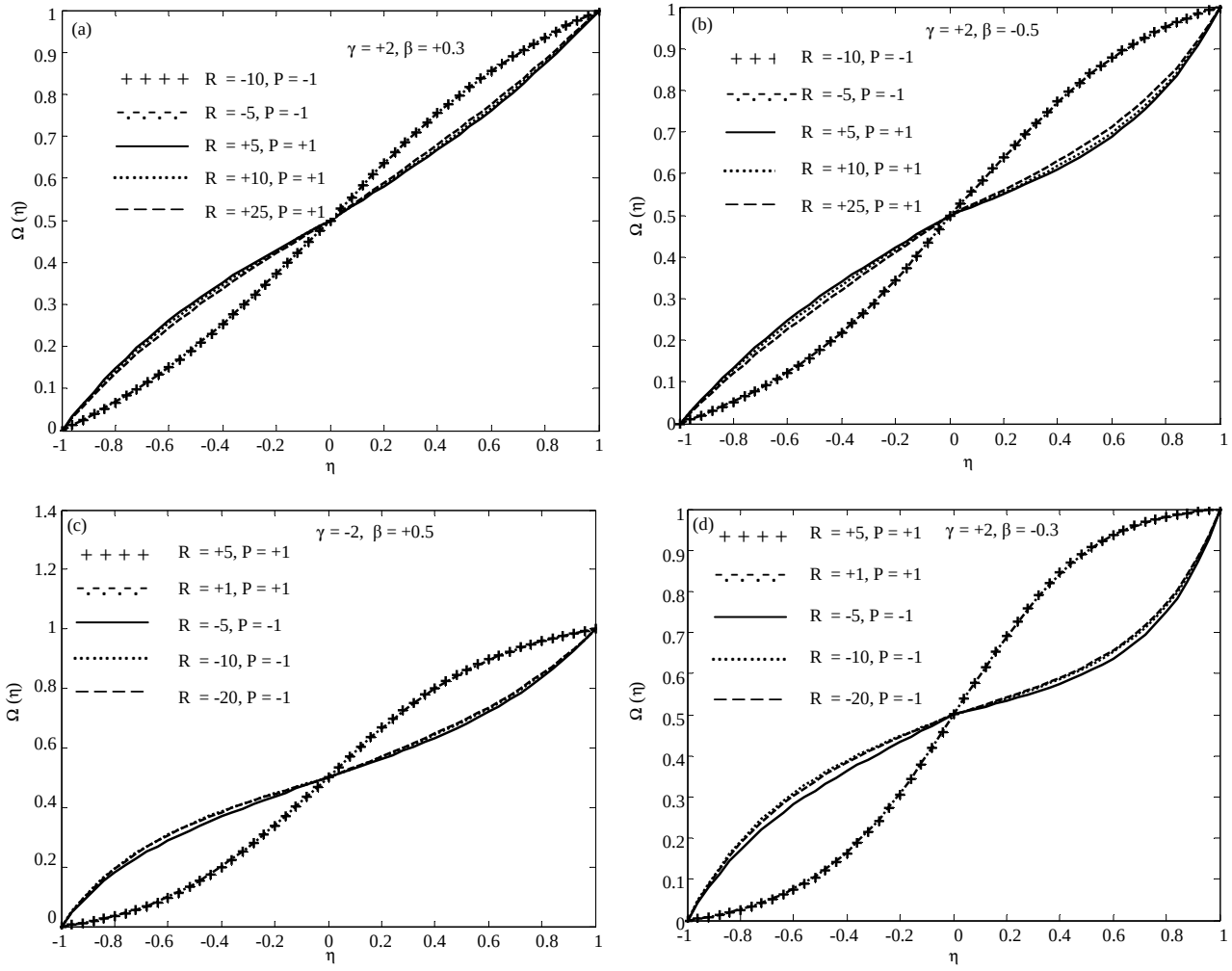


Fig. 5(a-d): Temperature under different suction/injection Reynolds numbers at P = ± 1, (a) For $\gamma$ =+2, $\beta$ = +0.3, (b) For $\gamma$ = +2, $\beta$ = -0.5, (c) For $\gamma$ = -2, $\beta$ = 0.5 and (d) For $\gamma$ = -2, $\beta$ = -0.3

Q($\eta$) and important oscillations are observed in the case of suction for positive accelerating parameters and in the case of injection for negative values of the parameter $\gamma$.

It appears from Fig. 5 that the variations of temperature are not very sensitive to the changes happening with respect to the suction Reynolds number at fixed $\gamma$, $\beta$ and P because for different negative values of R, function $\Omega$ is presented as a same constant curve. This observation is the same for different injection Reynolds numbers at fixed $\gamma$, $\beta$ and P. However, thermal behaviors differ by the sign of the Reynolds number since Fig. 5 shows that the curves corresponding to suction are well distinguishable from those corresponding to injection. Figure 6 shows that the Péclet number influences enough the distribution of temperature inside the channel. Indeed, the increase of the injection Péclet number at a fixed positive accelerating parameter gives the existence of a thermal boundary layer as shown in Fig. 6a. This thermal boundary layer which appears when the injection Péclet number approaches the value of 10 manifests itself as a horizontal large inflection area. Similarly, when the suction Péclet number approaches the value of -10, the thermal boundary layer takes place at a fixed negative accelerating parameter according to Fig. 6b. The curves that highlight the thermal boundary layer present two concavities. The first concavity situated in the region $-1<\eta<0$ is turned towards the stocking and the second concavity in the region $0<\eta<1$ is turned towards the top.

Despite the consideration of temperature-dependent thermal conductivity in this study, the results presented in light of Fig. 5 and 6 show that thermal behaviors are similar to those described in the case of constant thermal conductivity[27].

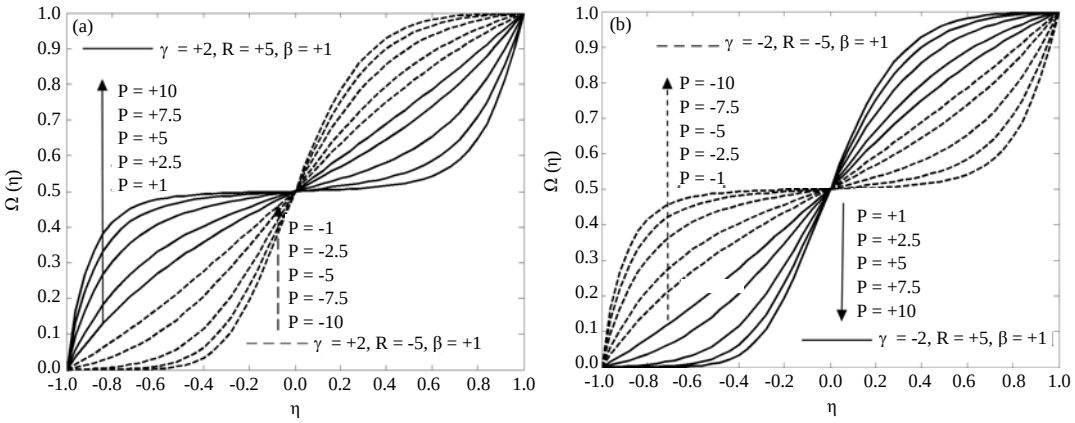


Fig. 6(a-b): Temperature under different suction/injection Péclet numbers at R = ± 5, (a) For $\gamma = +2$, $\beta = +1$ and (b) $\gamma = -2$, $\beta = +1$

## CONCLUSION

Fluid flow and heat transfer processes within a symmetric channel with two accelerating porous walls kept at different temperatures are modeled using the continuity, the Navier-Stokes and the energy equations. The solution is expressed in terms of a similarity variable for velocity components, as well as temperature. The results from the numerical integration show the dominance of the backward flow around the middle of the channel in the case of a fixed positive wall accelerating parameter. This backward flow also known as flow reversal diminishes with the increase of the injection Reynolds number and disappears in the case of a fixed negative wall accelerating parameter. Boundary layers take place inside the channel by increasing the injection Reynolds number while the parameter $\gamma$ is positive and with the growth of the suction Reynolds number at a negative fixed value of $\gamma$. These boundary layers induce inviscid injection and suction flows and cancel the oscillations of the normal pressure gradient within the flow domain. Thermal boundary layers which manifest themselves as large horizontal inflection areas within the channel occur when the injection Péclet number approaches the value of 10 at a fixed positive parameter $\gamma$ and when the suction Péclet number tends to -10 at a fixed negative accelerating parameter.

## REFERENCES


1. Xia, Z., 2014. Simulation and optimization of temperature characteristic of capacitive micromachined accelerometer system. J. Applied Sci., 14: 325-332.
2. Lim, F.Y., S. Abdullah and I. Ahmad, 2010. Numerical study of fluid flow and heat transfer in microchannel heat sinks using anisotropic porous media approximation. J. Applied Sci., 10: 2047-2057.
3. Sabeur-Bendehina, A., O. Imine and L. Adjlout, 2005. Optimization of the heat transfer rate in undulated enclosures with multiple partitions. J. Applied Sci., 5: 1237-1243.
4. Jalilvand, Z., F.Z. Ashtiani, A. Fouladitajar and H. Rezaei, 2014. Computational fluid dynamics modeling and experimental study of continuous and pulsatile flow in flat sheet microfiltration membranes. J. Membr. Sci., 450: 207-214.
5. Lee, M., B. Wang, Z. Wu and K. Li, 2015. Formation of micro-channels in ceramic membranes-spatial structure, simulation and potential use in water treatment. J. Membr. Sci., 483: 1-14.
6. Berman, A.S., 1953. Laminar flow in channels with porous walls. J. Applied Phys., 24: 1232-1235.
7. Wageman, W.E. and F.A. Guevara, 1960. Fluid flow through a porous channel. Phys. Fluids, 3: 878-881.
8. Tsangaris, S., D. Kondaxakis and N.W. Vlachakis, 2006. Exact solution of the Navier-Stokes equations for the pulsating Dean flow in a channel with porous walls. Int. J. Eng. Sci., 44: 1498-1509.
9. Griffond, J. and G. Casalis, 2001. On the nonparallel stability of the injection induced two-dimensional Taylor flow. Phys. Fluids, 13: 1635-1644.
10. Ferro, S. and G. Gnavi, 2000. Spatial stability of similarity solutions for viscous flows in channels with porous walls. Phys. Fluids, 12: 797-802.
11. Casalis, G., G. Avalon and J.P. Pineau, 1998. Spatial instability of planar channel flow with fluid injection through porous walls. Phys. Fluids, 10: 2558-2568.
12. Deka, R.K. and H.S. Takhar, 2004. Hydrodynamic stability of viscous flow between curved porous channel with radial flow. Int. J. Eng. Sci., 42: 953-966.
13. Moussy, Y. and A.D. Snider, 2009. Laminar flow over pipes with injection and suction through the porous wall at low Reynolds number. J. Membr. Sci., 327: 104-107.
14. Banks, W.H.H. and M.B. Zaturska, 1992. On flow through a porous annular pipe. Phys. Fluids A: Fluid Dyn., 4: 1131-1141.

15. Goto, M. and S. Uchida, 1990. Unsteady flows in a semi-infinite expanding pipe with injection through wall. Aeronaut. Space Sci. Jpn., 38: 131-138.
16. Chamkha, A.J., 1996. Solutions for fluid-particle flow and heat transfer in a porous channel. Int. J. Eng. Sci., 34: 1423-1439.
17. Hossain, M.A., S. Bhowmick and R.S.R. Gorla, 2006. Unsteady mixed-convection boundary layer flow along a symmetric wedge with variable surface temperature. Int. J. Eng. Sci., 44: 607-620.
18. Hona, J., E.N. Nyobe and E. Pemha, 2009. Dynamic behavior of a steady flow in an annular tube with porous walls at different temperatures. Int. J. Bifurcation Chaos, 19: 2939-2951.
19. Hona, J., E. Pemha and E.N. Nyobe, 2015. Viscous flow and heat transfer through two coaxial porous cylinders. Int. J. Multiphys., 9: 45-60.
20. Hona, J., E.N. Nyobe and E. Pemha, 2016. Creeping flow with non-uniform viscosity in a permeable industrial conduct. Int. J. Eng. Syst. Modell. Simul., 8: 183-194.
21. Dauenhauer, E.C. and J. Majdalani, 2003. Exact self-similarity solution of the Navier-Stokes equations for a porous channel with orthogonally moving walls. Phys. Fluids, 15: 1485-1495.
22. Fang, T. and J. Zhang, 2008. Flow between two stretchable disks-An exact solution of the Navier-Stokes equations. Int. Commun. Heat Mass Transfer, 35: 892-895.
23. Brady, J.F., 1984. Flow development in a porous channel and tube. Phys. Fluids, 27: 1061-1067.
24. Majdalani, J. and C. Zhou, 2003. Moderate-to-large injection and suction driven channel flows with expanding or contracting walls. J. Applied Math. Mech., 83: 181-196.
25. Sellars, J.R., 1955. Laminar flow in channels with porous walls at high suction Reynolds numbers. J. Applied Phys., 26: 489-490.
26. Wah, T., 1964. Laminar flow in a uniformly porous channel. Aeronaut. Quart., 15: 299-310.
27. Pemha, E., J. Hona and E.N. Nyobe, 2014. Numerical control of a two-dimensional channel flow with porous expanding walls at different temperatures. Int. J. Flow Control, 6: 119-134.